Supporting Information for:

CO_2 Hydrogenation to CH_3OH on Supported Cu Nanoparticles: Nature and Role of Ti in Bulk Oxides vs. Isolated Surface Sites

Gina Noh,[†] *Scott R. Docherty,*[†] *Erwin Lam,*[†] *Xing Huang,*[†,‡] *Deni Mance,*[†] *Jan L. Alfke,*[†] *Christophe Copéret**[,†]

† Department of Chemistry and Applied Biosciences and ‡ Scientific Center for Optical and Electron Microscopy, ETH Zürich, 8093 Zürich, Switzerland

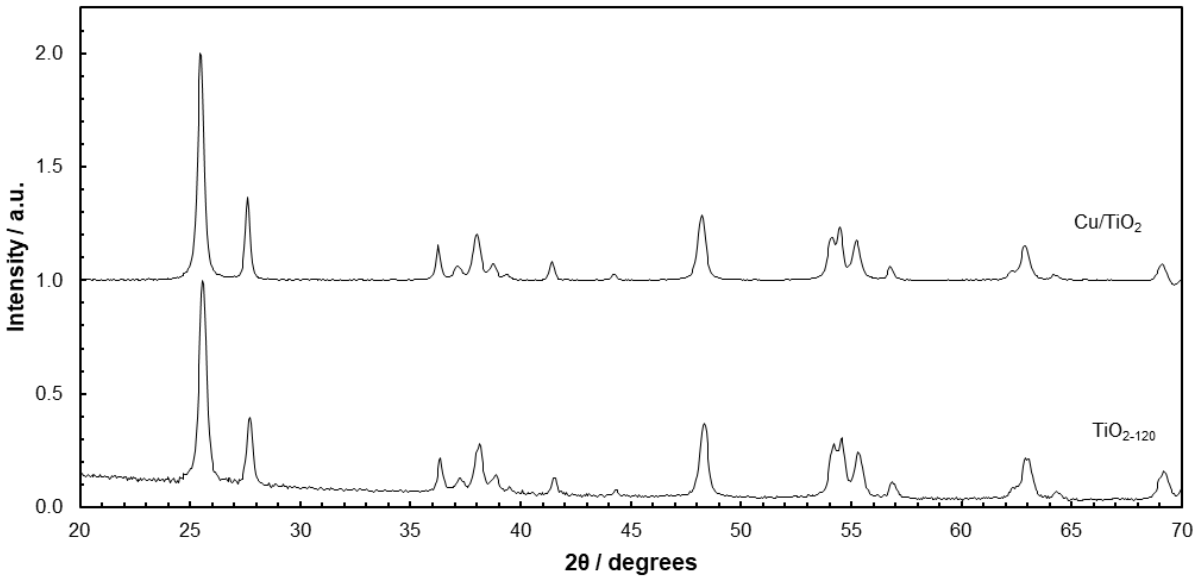

Figure S1. Powder X-ray diffraction patterns for $TiO_{2\text{-}120}$ (bottom; Degussa/Evonik P25) and Cu/TiO_2 (top). Patterns with and without Cu are identical, indicating that the TiO_2 support retains long-range order after dispersal of Cu nanoparticles and thermal treatments.

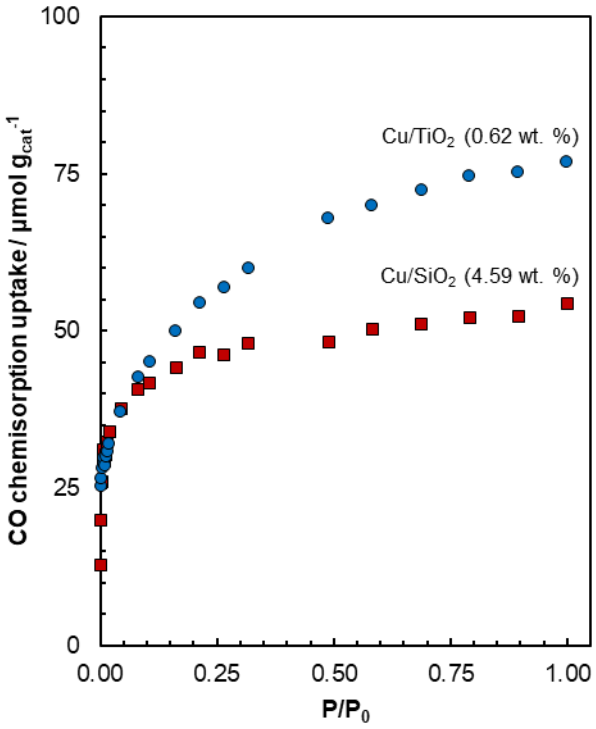

Figure S2. CO chemisorption isotherms for Cu/TiO_2 (blue) and Cu/SiO_2 (red) at 313 K. The specific CO uptake for Cu/TiO_2 is much greater than for Cu/SiO_2 in spite of having seven-fold less Cu per g_{cat} (0.62 wt. % vs. 4.59 wt. %).

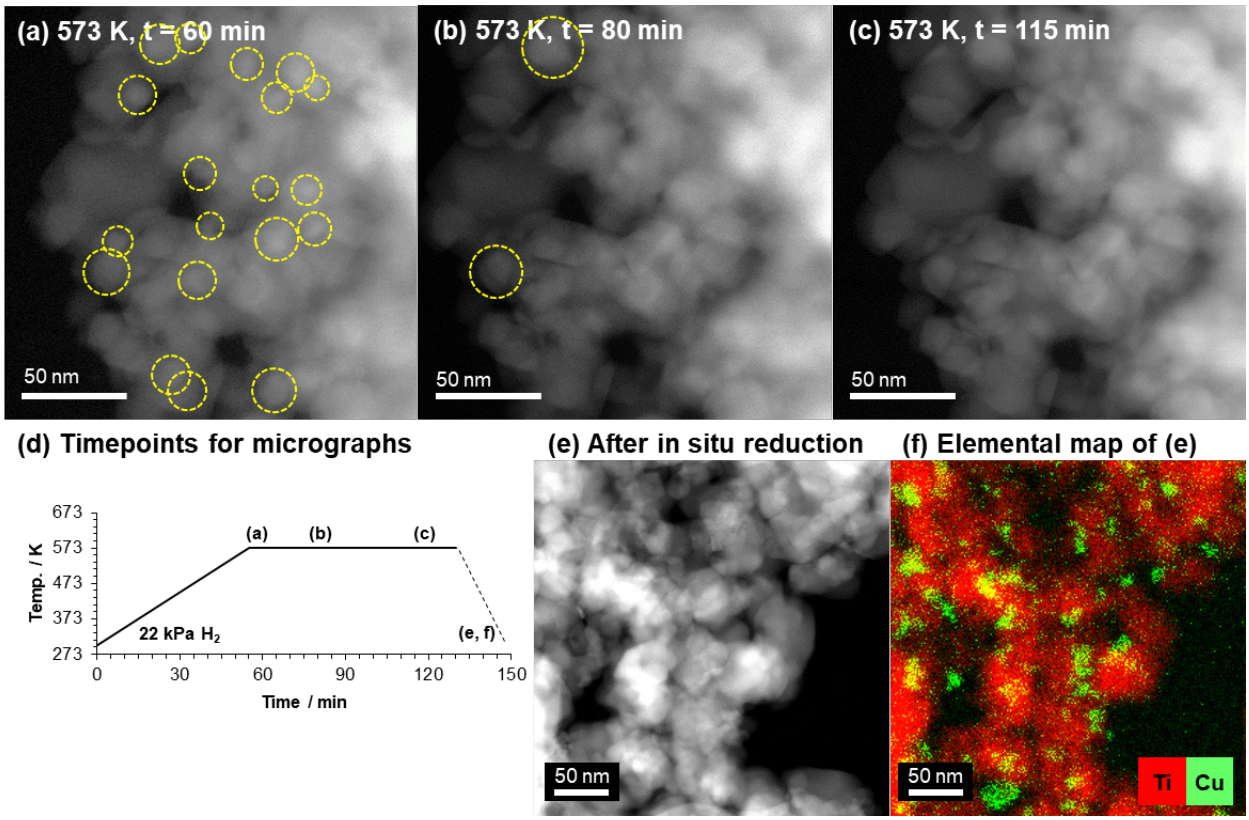

Figure S3. In situ reduction transmission electron microscopy experiment for Cu/TiO_2. Timepoints for representative micrographs, taken in the same spot with the shutter closed between images to avoid beam damage, are shown in **(a)**, **(b)**, and **(c)**. The yellow circles represent Cu particles where they remain discernible from the TiO_2 support. **(d)** Schematic of the conditions during in situ reduction experiments, indicating the timepoints for micrographs. **(e)** Representative micrograph after reduction, and **(f)** elemental mapping of (e) using EDX.

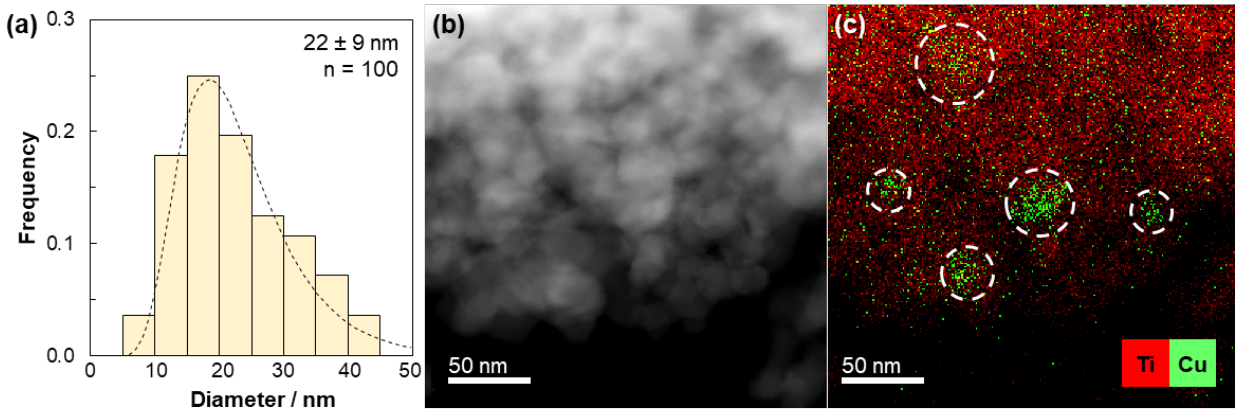

Figure S4. (a) Cu particle size histogram, **(b)** sample micrograph, and **(c)** elemental mapping using EDX, for Cu/TiO_2, introduced to the microscope under inert conditions. Dashed line in (a) represents the fitted log-normal distribution.

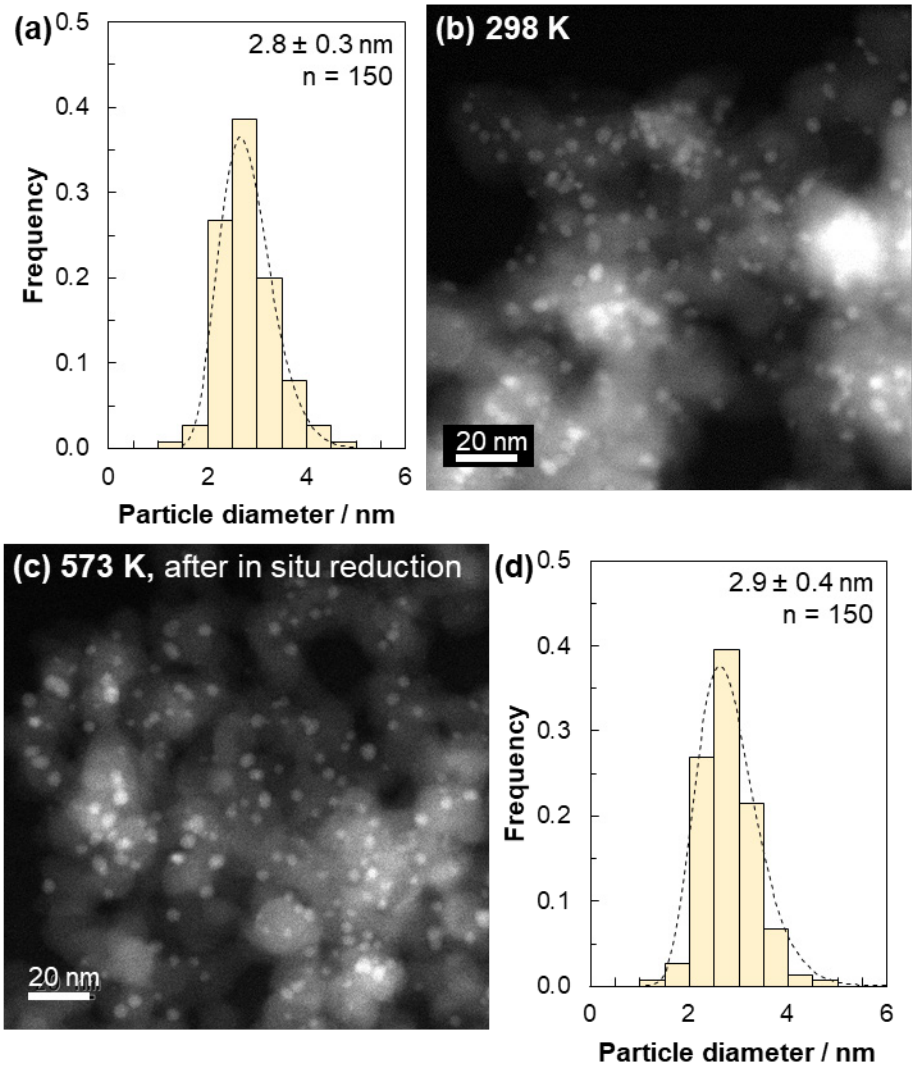

Figure S5. (a) Cu particle size histogram and **(b)** sample micrographs for Cu/SiO_2 exposed to air for >12 h prior to introduction to the microscope, and **(c)**, **(d)** after *in situ* reduction treatment (573 K (5 K min^{-1}) for 1 h, 22 kPa H_2, 0.16 cm^3 min^{-1}).

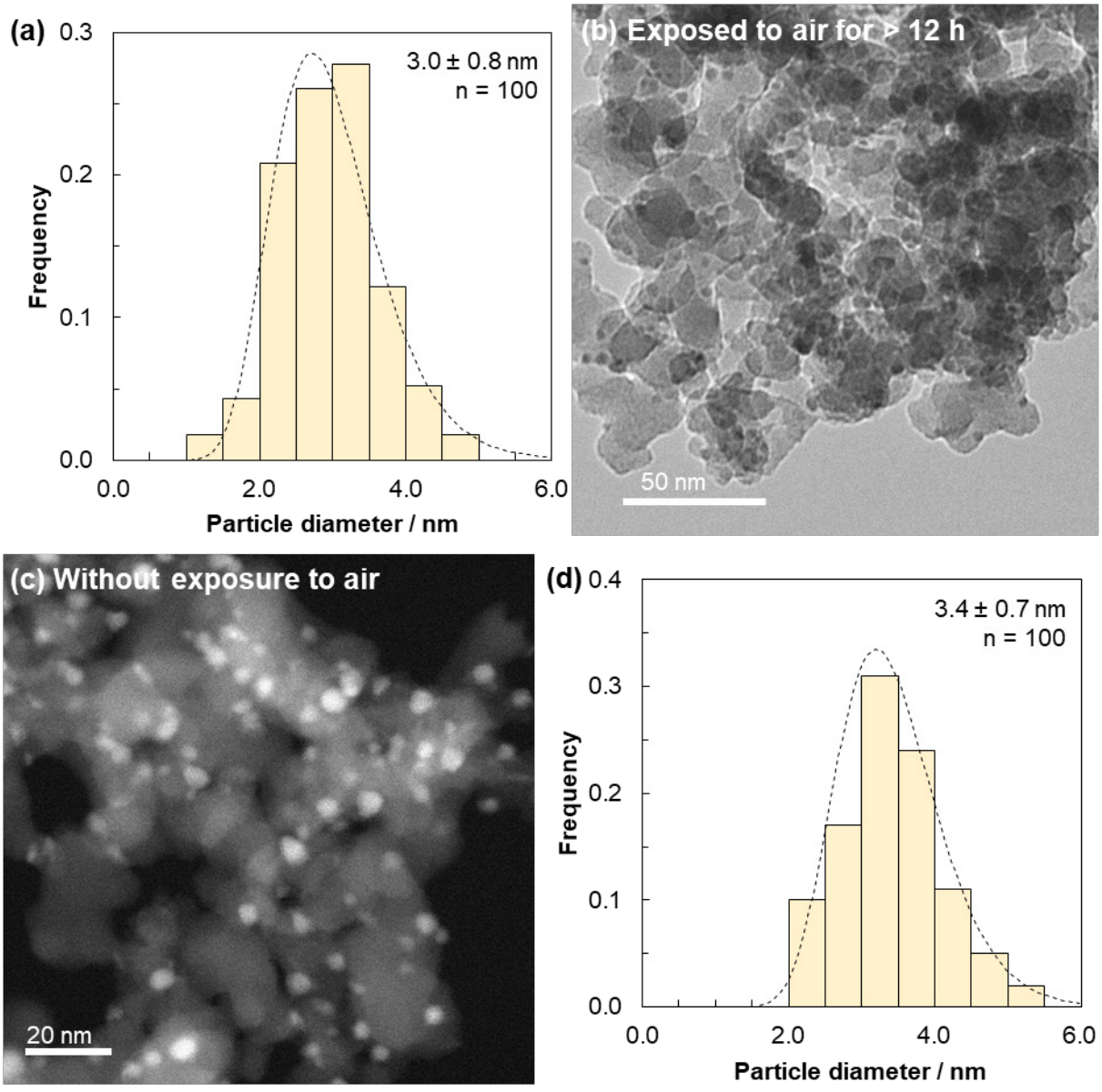

Figure S6. (a) Cu particle size histogram and **(b)** sample micrographs for Cu/TiO_x-SiO_2 exposed to air for >12 h prior to introduction to the microscope, and **(c)**, **(d)** for Cu/TiO_x-SiO_2 transferred to the microscope without exposure to air. Bright-field images were obtained using a Hitachi HT7700 microscope (100 kV).

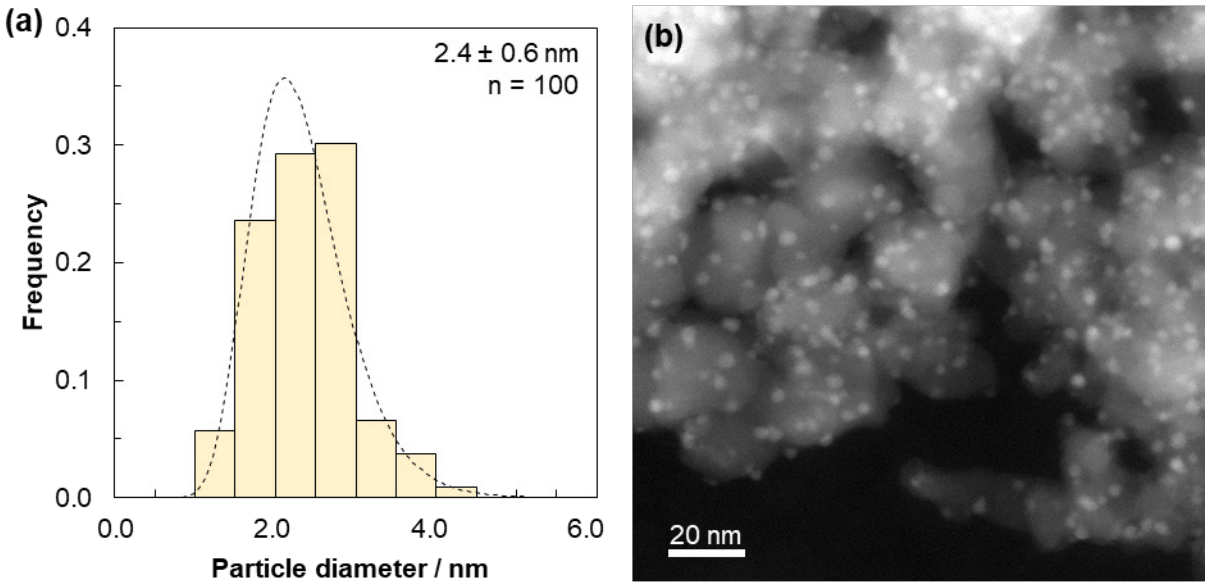

Figure S7. (a) Cu particle size histogram and **(b)** sample micrographs for $Cu/Ti_2@SiO_2$ transferred to the microscope without exposure to air.

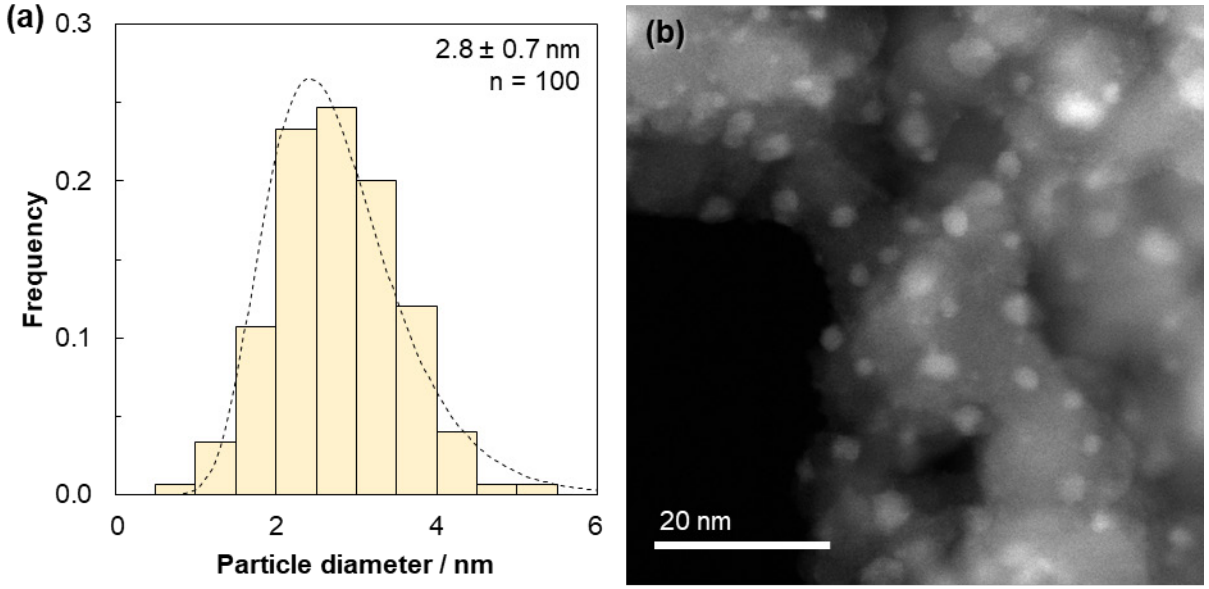

Figure S8. (a) Cu particle size histogram and **(b)** sample micrographs for $Cu/Ti@SiO_2$ transferred to the microscope without exposure to air. Micrographs of the materials exposed to air are included in previous work.[1]

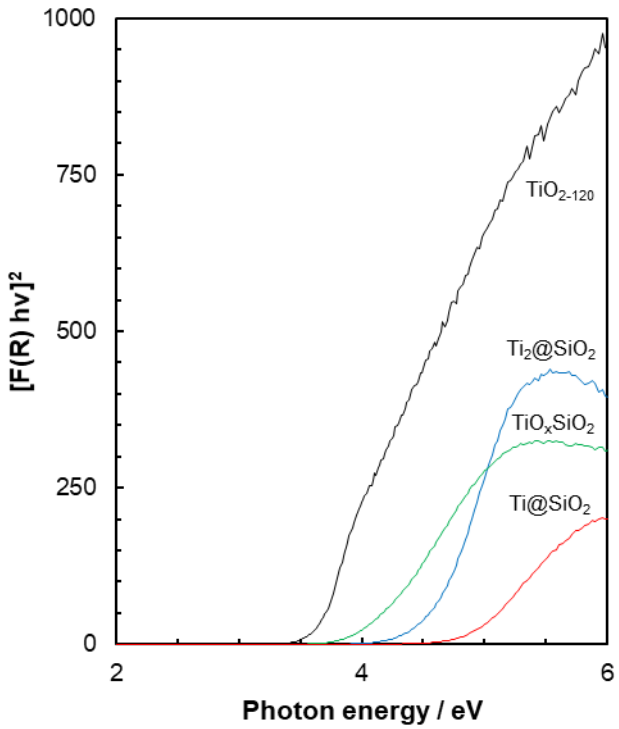

Figure S9. Tauc plot for Ti-containing supports. Values of the optical bandgap were obtained by extrapolating the linear region of the curves to zero $[F(R)\ h\nu]^2$ values and are included in Table 1 of the main text.

Section S10. Grafting and thermal treatment of a Ti^{III} precursor on SiO_2.

To examine the stability of Ti^{III} metal centers dispersed on SiO_2, a Ti^{III} precursor ($Ti(OSi(O^tBu)_3)_3$, prepared according to literature procedures[2]) was grafted onto $SiO_{2\text{-}700}$ then thermally treated. The material was examined using EPR spectroscopy (Figure S10). A solution of $Ti(OSi(O^tBu)_3)_3$ in toluene (0.15 mmol; 20 mL) was added to a slurry of $SiO_{2\text{-}700}$ (1 g) in toluene (10 mL) then stirred for 12 h; the slurry was allowed to settle, then the supernatant was decanted. The material was rinsed three times with toluene then dried under vacuum (~10^{-3} Pa) at room temperature, followed by treatment under vacuum (~10^{-3} Pa) at 773 K (0.083 $K.s^{-1}$) for 5 h.

The prominent EPR signal for Ti^{III} (g = 1.96) disappears after thermal treatment. This suggests that the small amounts of water generated during decomposition of (O^tBu) ligands during thermal treatments are sufficient to oxidize Ti^{III} to Ti^{IV}, essentially irreversibly. The EPR spectrum for the material treated under reducing conditions (under H_2 flow (101 kPa) at 773 K (0.083 $K.s^{-1}$) for 5 h) is identical to the spectrum for the material treated under vacuum.

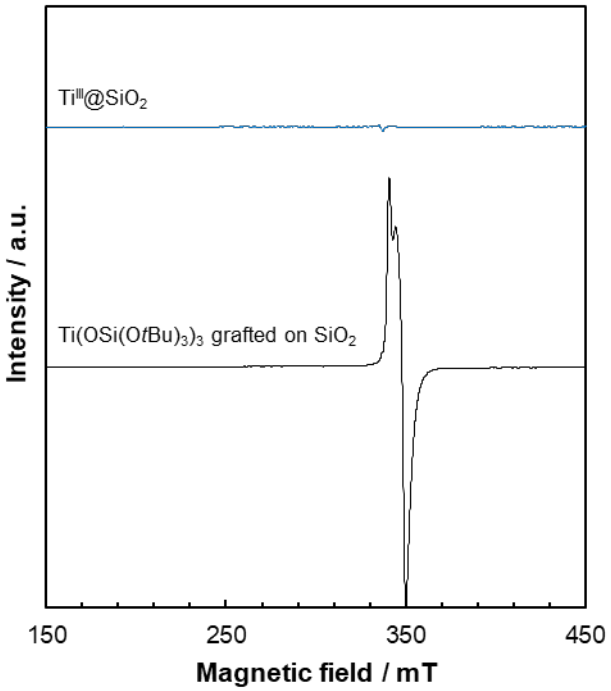

Figure S10. EPR spectra (100 K, X band) of $Ti(OSi(O^tBu)_3)_3$ grafted on SiO_2 (bottom) and after thermal treatment (top).

Section S11. Supplemental catalytic reaction data

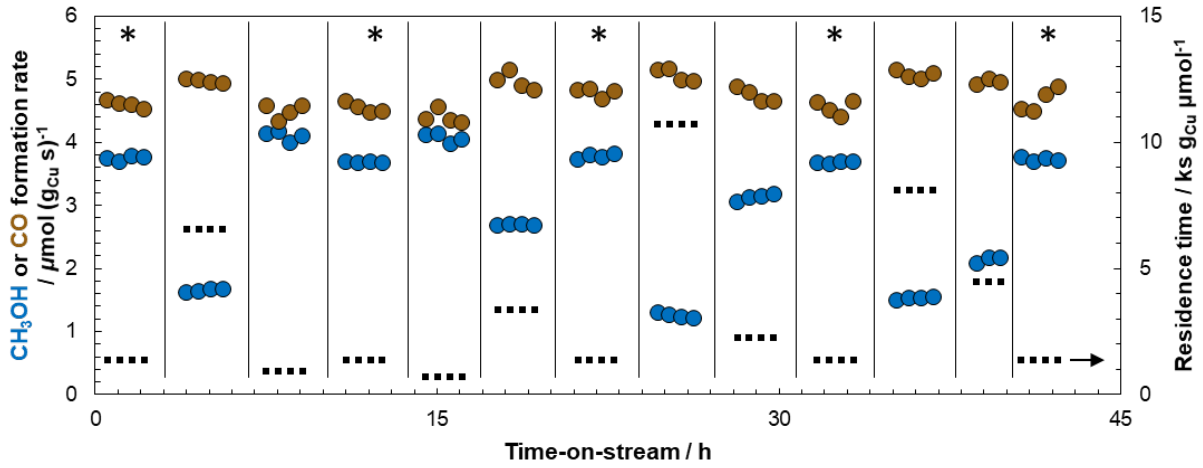

Figure S11. CH_3OH (blue, left axis) and CO (brown, left axis) formation rates and CO_2 residence time (black, right axis) as a function of time-on-stream for CO_2 hydrogenation reactions on Cu/SiO_2 (503 K, 2.5 MPa total pressure; 1:3:1 CO_2:H_2:Ar).
* Reference conditions used to monitor catalyst deactivation as a function of time-on-stream.

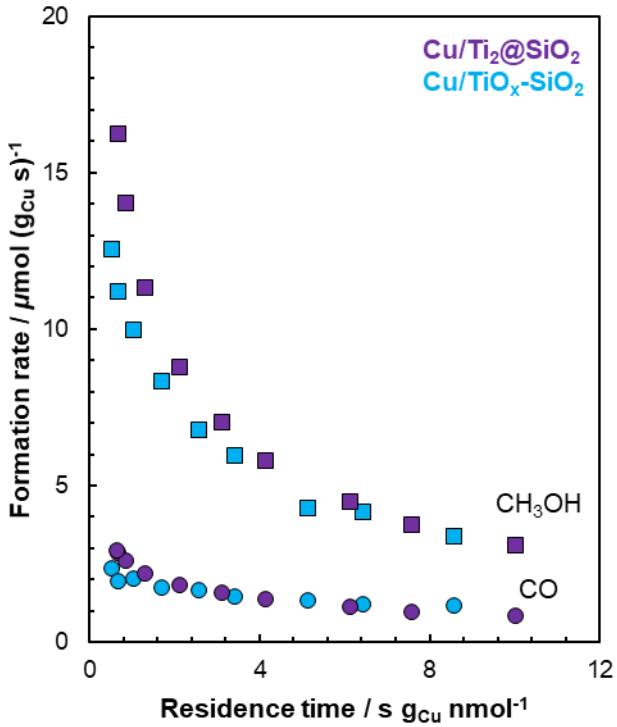

Figure S12. CH_3OH (squares) and CO (circles) formation rates as a function of CO_2 residence time for $Cu/Ti_2@SiO_2$ and Cu/TiO_x-SiO_2 (503 K, 2.5 MPa total pressure; 1:3:1 CO_2:H_2:Ar).

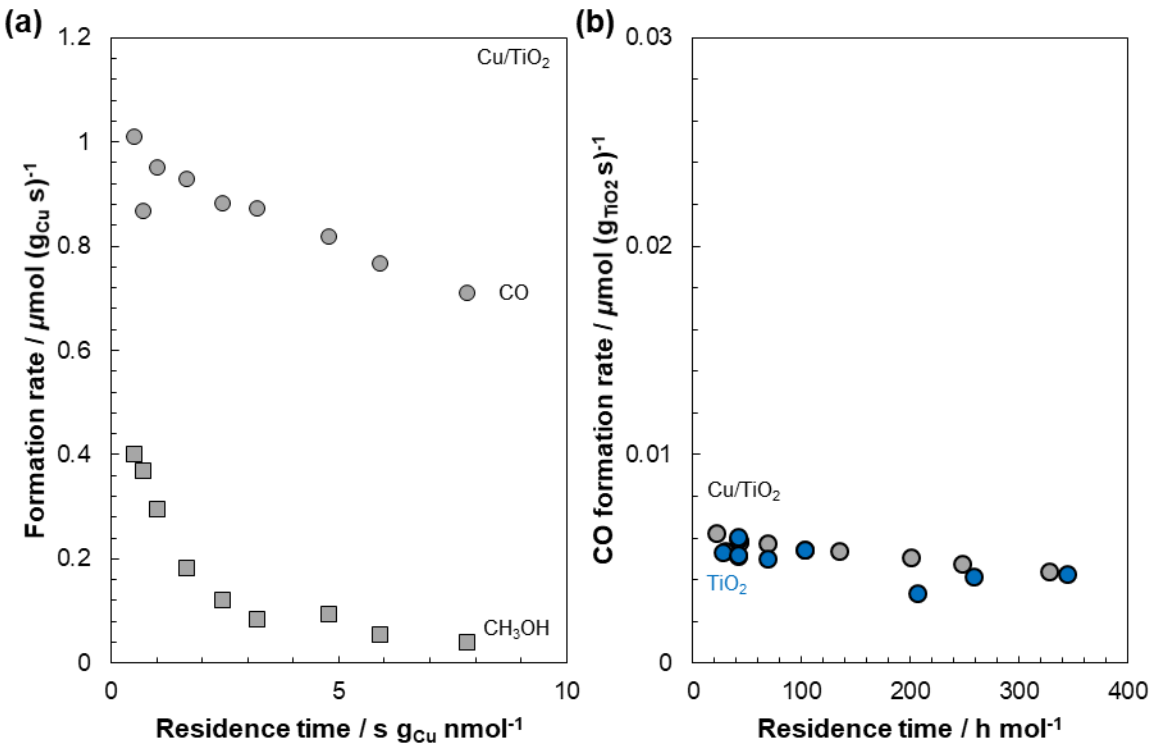

Figure S13. (a) CH_3OH (squares) and CO (circles) formation rates on Cu/TiO_2, normalized by mass of Cu. CO formation rates include contributions from the support. **(b)** CO formation rates, normalized by the mass of TiO_2, on Cu/TiO_2 (grey) and TiO_2 (blue). 503 K, 2.5 MPa total pressure; 1:3:1 CO_2:H_2:Ar.

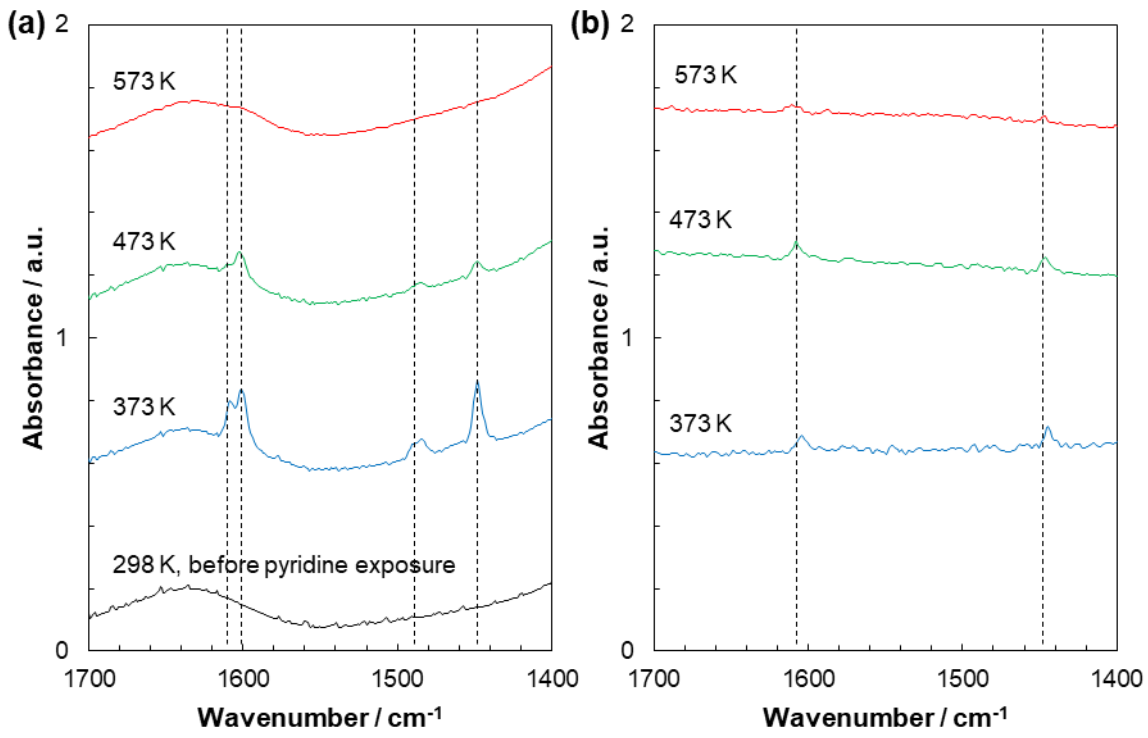

Figure S14. (a) Transmission IR spectra for Cu/Ti@SiO_2 and **(b)** ATR IR spectra for Cu/TiO_2 after exposure of the sample to pyridine (0.2 Pa at 298 K for 5 min), followed by evacuating (~10^{-3} Pa) at 373 K (blue line), 473 K (green line), and 573 K (red line) for 15 minutes. Dashed lines highlight pyridine vibrational bands.

References

(1) Noh, G.; Lam, E.; Alfke, J. L.; Larmier, K.; Searles, K.; Wolf, P.; Copéret, C. Selective Hydrogenation of CO_2 to CH_3OH on Supported Cu Nanoparticles Promoted by Isolated Ti^{IV} Surface Sites on SiO_2. *ChemSusChem* **2019**, *12* (5), 968–972.

(2) Allouche, F. Structure – Activity Relationship in Olefin Polymerization with Well-Defined Ti(III) and Ln(II) Molecular and Surface Complexes, ETH Zurich, 2018.